ELSEVIER

Journal of Nuclear Materials 307–311 (2002) 1471–1477

journal of nuclear materials

www.elsevier.com/locate/jnucmat

Helium and hydrogen generation in pure metals irradiated with high-energy protons and spallation neutrons in LANSCE

B.M. Oliver [a,*], M.R. James [b], F.A. Garner [a], S.A. Maloy [b]

[a] *Pacific Northwest National Laboratory, P.O. Box 999, Richland, WA 99352, USA*
[b] *Los Alamos National Laboratory, Los Alamos, NM 87545, USA*

Abstract

High-power spallation neutron sources will require accurate estimates of cross-sections for generation of He and H in structural materials. At high-proton energies, very high levels of gas atoms are generated in all constituents of typical iron-based and nickel-based structural alloys, with He typically ~150 appm/dpa and H at levels ~3–5 times higher. Improved estimates of these cross-sections have been derived from a series of irradiations conducted at relatively low temperatures (<100 °C) in the Los Alamos Neutron Science Center as part of a test program supporting the Accelerator Production of Tritium Program. Pure metal dosimetry foils were irradiated in two different spectra ranging from ~800 MeV protons to a mixed distribution of both protons and spallation neutrons. Most of the gas production was due to spallation reactions with the proton beam, although gas and especially damage production from lower-energy spallation neutrons became more significant at the mixed proton/neutron location. The measured He concentrations are similar to those derived in other proton environments, but larger by about a factor of two than those calculated using the LAHET/MCNPX code system. Unlike He, the measured H retention levels are affected by diffusional losses, but H is still retained at rather high concentrations, allowing a lower bound estimate of the H generation cross-sections. Published by Elsevier Science B.V.

1. Introduction

Structural materials exposed to mixed spectra of high-energy protons and lower-energy spallation neutrons found in accelerator-driven spallation neutron sources must withstand the intensive generation and retention of large levels of helium and hydrogen. Confident prediction of these generation rates requires their measurement at high exposure, but very little data are available at high-displacement levels.

The Accelerator Production of Tritium (APT) project [1] was proposed as one of several solutions to the US National need for tritium. In the APT concept, high-energy protons would impinge on a tungsten target producing high-energy spallation neutrons. An important technical issue was the potentially strong impact of radiation damage and transmutant production on structural materials resulting from the mixed proton and neutron distributions expected in the facility.

To address this issue, a series of irradiations were conducted in the Los Alamos Neutron Science Center (LANSCE) supporting the APT program [2]. In these irradiations, a variety of candidate structural alloys and pure dosimetry foils were placed in various particle spectra, ranging from ~800 MeV protons, to mixed energy distributions of both protons and spallation neutrons, and finally to distributions consisting primarily of high-energy neutrons. Specimen irradiation temperatures in the LANSCE test were 200 °C or less, with most below 100 °C.

At proton energies on the order of hundreds of MeV, high levels of gas atoms are generated in constituents of typical structural alloys, with helium typically ~80–160 appm/dpa, and hydrogen (i.e., protium) at levels approximately an order of magnitude higher [3]. Protons generated from the spallation reactions exist in two

* Corresponding author. Tel.: +1-509 376 9228; fax: +1-509 372 2156.
E-mail address: brian.oliver@pnl.gov (B.M. Oliver).

0022-3115/02/$ - see front matter Published by Elsevier Science B.V.
PII: S0022-3115(02)01295-3

roughly equal distributions, the first with energies of the order of ~100 MeV from the internuclear cascade, and the second with energies of ~1 MeV from the subsequent nuclear evaporation event. For the typical size of specimens employed in the APT irradiation program, the large range of the high-energy proton component results in their near-total loss from the irradiated volume while a significant fraction of the evaporation protons are stopped in the specimens (note that some of the high-energy protons may also recoil into adjacent samples). Thus, for in-beam specimens ~50% or less of the total generated hydrogen is expected to come to rest in the specimens. On the other hand, >95% of the heavier helium generated at lower energies is expected to be retained in the specimens. Additionally, since the specimens in this experiment were covered by adjacent specimens or foil covers, helium fluxes across surfaces of adjacent samples nearly cancel, leading to very little net loss.

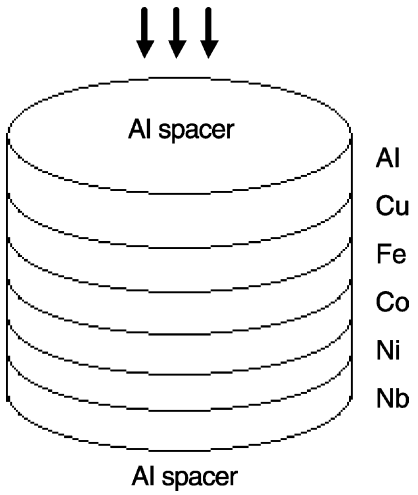

Fig. 2. Schematic diagram of dosimeter foil package.

2. Experimental conditions

A diagram of the experimental setup in the LANSCE facility is shown in Fig. 1. At the front of the experimental assembly the 1 mA, ~800 MeV proton beam was roughly Gaussian in distribution, with a 2σ width of ~30 mm. The proton energy spectrum then degrades with depth into the experimental assembly. Details of the sample configurations and proton/neutron spectra have been provided elsewhere [4].

The thin (0.05–0.4 mm) dosimetry foils were mounted in packets, each containing six disks, 3 mm in diameter, of Al, Cu, Fe, Co, Nb and Ni, as shown in Fig. 2. These packets were mounted in thin foil-covered blades with metal-to-metal contact for optimum cooling, with high-velocity water flowing between the various blades. The foils chosen for the present measurements were irradiated in tube 1, the first tube in the leading experimental array. The foils were from position 5 at −1.4 cm from the beam center, and position 13 at the edge of the array at +4.2 cm. They had different relative amounts of proton and neutron fluxes, and therefore different cumulative dpa levels, averaging ~8 and ~0.8 dpa, respectively. Calculated temperatures of the foils ranged from ~35 °C at the 0.8 dpa location, to ~100 °C at the 8 dpa location.

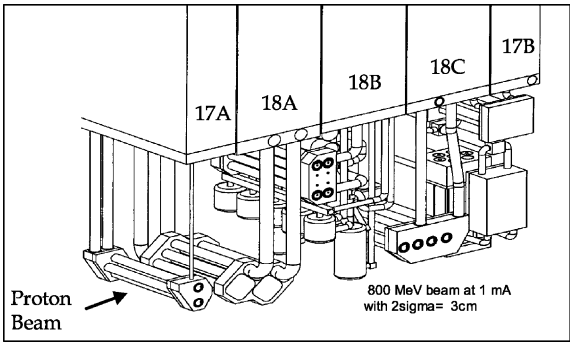

Fig. 1. APT irradiation set-up in the LANSCE Irradiation Facility. The specimens discussed in this paper were irradiated in assembly 18C (tube 1).

3. Gas analyses

Specimens for gas analysis were cut from each of the foil samples. Each of the helium analysis specimens was etched to remove ~0.013 mm of surface material. This etching step was done to remove material that may have been affected by α-recoil either out of the sample or into the sample from the adjacent foils. The hydrogen analysis specimens were cut in a similar manner from unetched sections of the original samples to avoid potential introduction of hydrogen by the etching process.

3.1. Helium analysis system

Helium analyses were conducted by gas mass spectrometry at Pacific Northwest National Laboratory (PNNL). Details of the analysis system have been presented elsewhere [5]. Helium contents were determined by vaporizing each sample in a resistance-heated crucible in a high-temperature vacuum furnace. The concentrations of the two helium isotopes were determined either by direct measurements of the mass spectrometer signal for ^{3}He or ^{4}He, or by an isotope-dilution technique where the released helium is compared with a known quantity of added 'spike' of the other isotope.

Reproducibility of the analysis system for samples with known homogeneous helium content is ~0.5%. Absolute accuracy has been determined in many previous studies to be generally better than 1%.

3.2. Hydrogen analysis system

Hydrogen analyses were conducted using a separate mass spectrometry system at PNNL [6]. The system is based on a low-volume extraction crucible in combination with a quadrupole detector. The system has a detection limit of ~1 appm for steel, and an absolute accuracy of ~20% or better. Sample analyses are conducted by sequentially dropping individual specimens into the heated crucible. Hydrogen release is measured as a function of time, with total hydrogen determined from the integral of the release curve.

4. Predictions of gas generation

Details of the dosimeter foils analyzed are given in Table 1, along with predictions of the total helium and hydrogen gas generations (appm) and damage (dpa) using LAHET/MCNPX (LCS) [7,8]. Calculations were performed using either LAHET 2.8.3 or MCNPX 2.1.6, which employs the LAHET physics model for proton interactions. Calculated-to-experimental (C/E) values apply to either code. The fluences at these foil locations were quantified using the spallation/transmutation productions measured in the same foils, followed by a standard dosimetry analysis [4] for the combined proton and neutron fluences. Cross-sections for He, H and dpa production in the foil materials were calculated using default settings for the physics parameters with the exception of the pre-equilibrium option being turned on. This includes the use of the GCCI level-density parameters [9,10], which have previously been shown to give erroneous values for He generation in mid-Z elements [11]. With this data, the fluences and cross-sections were combined to provide the He, H and dpa estimates for each foil material. The predicted hydrogen contents include energetic losses from higher-energy protons, but do not include any estimate of diffusional losses.

5. Gas analysis results and discussion

5.1. Helium generation

Helium analyses were conducted on five of the six dosimeter foils in each of the foil packets, and the results are given in Table 2. The Nb foils were not measured as they were destructively analyzed as part of the dosimetry analysis. Helium generation rates for Fe, Ni, and Cu averaged about 170 appm/dpa, and are in excellent agreement with rates observed earlier for various alloys from the APT program [12]. Generation rates for Cu were slightly lower at ~140 appm/dpa, and those for Al were somewhat higher at ~300 appm/dpa. The most significant observation is that the measured helium generation rates are significantly higher than expected based on the LCS calculations. This is a rather general problem as noted by Enke et al., where measured helium cross-sections for Fe and Ni are larger than predicted by the INCL, LAHET, MCNPX, and HERMES code systems over a wide range of energies [13].

The earlier study by Green [3] using HETC, a predecessor to LCS, gave measured and calculated values for iron and nickel at 750 MeV that agree with the

Table 1
Dosimetry foil samples and MCNPX predictions

Sample	Material and purity (%)	Thickness (mil)	Foil stack[a]	Protons (p/cm^2)	MCNPX predictions		
					Dose[b] (dpa)	Gas concentration (appm)[c]	
						He	^{1}H
C81	Al-99.9974	5	1-5-13	1.58×10^{20}	0.64	40.1	107
C85	Cu-99.9928	5			~0.8	39.6	326
C82	Fe-99.987	5			1.02	37.1	329
C83	Co-99.896	2			~0.8	41.0	385
C84	Ni-99.837	3			0.75	42.0	356
C86	Al-99.9974	5	1-5-5	2.47×10^{21}	3.4	614	1537
C90	Cu-99.9928	5			8.2	605	4870
C87	Fe-99.987	5			8.7	574	4946
C88	Co-99.896	2			8.4	623	5698
C89	Ni-99.837	3			9.5	644	5354

[a] Tube-envelope-ID.
[b] Dose uncertainty is ~5–10%, except for the low-dose Cu and Ni, where the uncertainty is somewhat higher (perhaps 10–15%).
[c] Concentration uncertainty is ~4% for the He and ~3% for the H.

Table 2
Measured helium in dosimetry foils

Sample	Material	Mass[a] (mg)	Measured helium						
			10^{14} atoms		$^4He/^3He$ ratio	Total[b] (appm)	(appm/dpa)		
			He^3	He^4			Measured	Calculated	C/E
C81	Al	0.135	0.299	2.306	7.70	86.49	138	62.9	0.45
		0.177	0.417	3.184	7.64	90.13			
C82	Fe	0.424	0.820	3.879	4.73	102.2	131	50.9	0.39
		0.667	1.22	5.829	4.76	98.07			
		0.385	0.883	3.480	3.94	105.2[c]			
C83	Co	0.120	0.168	1.139	6.77	106.6	134	46.4	0.35
		0.236	0.335	2.264	6.76	107.8			
C84	Ni	0.286	1.23	3.198	2.61	150.9	188	54.4	0.29
		0.692	2.78	6.693	2.41	133.5			
		0.200	0.833	2.065	2.48	141.2			
C85	Cu	0.530	0.514	4.100	7.98	91.83	126	52.5	0.42
		0.720	0.811	6.524	8.04	107.5			
		0.362	0.392	3.135	7.99	102.8			
C86	Al	0.340	10.5	76.27	7.28	1143	319	178	0.56
		0.398	11.4	82.76	7.29	1060			
C87	Fe	0.502	10.1	66.03	6.51	1407	172	74.1	0.43
		0.636	12.7	83.62	6.58	1405			
C88	Co	0.266	4.69	33.99	7.25	1423	160	65.5	0.41
		0.390	6.72	48.58	7.23	1388			
C89	Ni	0.207	3.94	26.53	6.74	1435	168	73.9	0.44
		0.407	7.53	50.88	6.76	1398			
C90	Cu	0.882	12.4	97.32	7.82	1312	136	67.8	0.50
		1.273	17.6	136.6	7.76	1278			

[a] Mass of analysis specimen. Mass uncertainty is ±0.002 mg.
[b] Total helium concentration in atomic parts per million (10^{-6} atom fraction) with respect to the total number of atoms in the specimen.
[c] Measurement conducted in August 2001. All other measurements were conducted in April 2000.

present measured values, but it is not known what physics settings were employed in the then-current version of HETC.

As expected, significant levels of ^3He were also seen in the foils, with helium 4/3 ratios ranging from ~3 to 8. One surprising result, however, is that the helium 4/3 ratios are lower than expected, particularly in the Fe and Ni at the lowest exposure of 0.8 dpa. The previous measurements in LANSCE for higher-Z materials [3] showed 4/3 ratios, ranging from ~8 for Fe and Ni to ~14 for W. The iron and nickel foils at the highest exposure in the present experiment had 4/3 ratios of 6.6 and 6.7, respectively.

Protons produce most of the ^3He, whereas ^4He is produced by both protons and neutrons. Therefore, one would have expected the 4/3 ratio to *increase* as one gets further away from the proton beam. The reason for the lower 4/3 ratios is now suspected to be from spallation-formed tritium (and subsequent decay to ^3He). As is shown in Table 2, recent measurements show a decrease in the 4/3 ratio in the low-dose Fe with time, from ~4.7 measured in April 2000 to ~3.9 in August 2001. Analysis of this data would suggest that this trend could be explained by a tritium content in the material at end of irradiation of about 40 appm. This would represent a ^3H to ^4He generation ratio of about 0.5, which is somewhat higher than predicted by LAHET/MCNPX, but still within possible uncertainty in the model calculations. The other pure metals (Al, Co, Cu) had helium 4/3 ratios of 7.3, 7.2 and 7.8, respectively, at the higher exposure level of ~8 dpa. The values at the lower exposure of 0.8 dpa were remarkably similar at 7.7, 6.8 and 8.0, all well within experimental error. The increase in 4/3 ratio from 0.8 and 8 dpa in this mixed spectra experiment, and then to the higher values of Green's monoenergetic proton study, suggests that there may be an

increase of the He 4/3 ratio with increasing proton energy, however, this may also be an artifact of tritium generation and decay.

Hydrogen measurements on the dosimetry foils are given in Table 3 along with the LCS predictions. Note that the original measured values (columns 5 and 6) include contributions from hydrogen present in the unirradiated material. These hydrogen levels were measured and showed average values of Al, 91 appm; Al, 140 appm; Fe, 186 appm; Co, 112 appm; Ni, 112 appm; and Cu, 116 appm. The measured hydrogen-to-dpa ratios listed have been corrected for these background levels. Note that the post-irradiation retained hydrogen varies rather strongly with the metal, and in some case, is variable from specimen to specimen. The differences in hydrogen retention within each foil packet do not follow known trends related to solubility or diffusion of hydrogen in various metals and alloys, and probably reflect different trapping types and densities induced by radiation in each alloy or metal. Except for Al, the high-exposure foils have lower retained H/dpa ratios than the low-exposure foils. This is probably due in part to the fact that the high exposure foils were at a higher temperature during the irradiation (~100 °C versus ~35 °C), thereby increasing diffusional losses. Other possible explanations include the fact that the lower-energy protons are more easily retained in the samples, or synergism of efficient displacement production combined with low-energy proton production.

Table 3
Retained hydrogen in APT dosimetry foils.

Sample	Material	Analysis temperature[a] (°C)	Mass[b] (mg)	Measured hydrogen				
				(10^{15} at.)	(appm)[c]	(appm/dpa)		
						Measured[d]	Calculated	C/E
C81	Al	600	0.475	2.27	214	207	168	0.81
			0.552	2.86	232			
C82	Fe	1200	2.062	25.4	1140	1331	418	0.31
			1.641	21.5	1210			
C83	Co	1200	0.817	6.79	813	770	411	0.53
			1.281	10.4	790			
C84	Ni	1200	1.098	36.0	3190	3983	510	0.13
			1.254	39.1	3040			
C85	Cu	870	0.948	4.87	330	724	445	0.61
			1.408	14.2	1060			
C86	Al	600	0.322	14.3	1990	540	445	0.82
			0.538	23.0	1920			
C87	Fe	1200	1.717	235	12 700	1131	597	0.53
			1.920	150	7270			
			1.107	60.7	5080			
			1.323	177	12 400			
C88	Co	1200	0.610	16.5	2640	410	564	1.38
			0.766	45.9	5870			
			0.575	19.7	3360			
			0.629	20.9	3260			
C89	Ni	1200	0.828	54.9	6460	588	675	1.15
			1.246	61.2	4780			
			0.738	31.7	4190			
			0.838	41.7	4850			
C90	Cu	870	1.001	13.2	1390	130	564	4.35
			1.168	14.4	1300			

[a] Temperature of system crucible.
[b] Mass of specimen for analysis. Mass uncertainty is ±0.002 mg.
[c] Hydrogen concentration in atomic parts per million (10^{-6} atom fraction) with respect to the total number of atoms in the specimen.
[d] Hydrogen values have been corrected for measured hydrogen in unirradiated control material (see text).

In general, the retained hydrogen levels measured in Co and Ni are consistent with measurements reported earlier on alloys from the APT program at similar dpa levels [12,14]. The retained hydrogen values are generally within a factor of two of those calculated. There is also a clear trend of increasing C/E with dpa, again suggesting increased diffusional losses for the high-dose (higher-temperature) samples. The exceptions are the low-dose Ni, and to a lesser extent Fe, and the high dose Cu. In the case of Ni, the retained H was significantly higher than predicted, whereas for Cu is was significantly lower. For Ni, the higher value could be due to enhanced trapping as was observed in earlier measurement of Alloy 718 from the same experiment [12]. The hydrogen retention rate in Fe is about twice as high as was observed earlier in 9Cr–1Mo. There may also be some bias in several of the hydrogen measurements related to recoil from adjacent foils. Note in Fig. 2 that there are significant differences in atomic number of adjacent specimens in two cases, Al/Cu and Ni/Nb. Since the spallation-produced protons have larger ranges than do alpha particles, and proton generation is sensitive to atomic number, there is a higher probability of 'cross-talk' between specimens, leading to possible skewing of the retained hydrogen that is not related to solubility.

6. Conclusion

This study has shown that measured helium generation rates of mid-Z elements are larger by roughly a factor of two compared to those calculated by LAHET/MCNPX. This indicates that separate physics parameters are required for each range of atomic numbers. Also, differences in the present predictions and those earlier of Green indicate that the current LCS physics model is not accurate for the prediction of helium production in these materials. The ratio of ^{4}He/^{3}He generation may be somewhat sensitive to proton energy, increasing as the proton energy increases, however, additional study is required to separate such an effect from potential tritium generation and decay. User knowledge of the calculational models and of data in the field are critical in determining a helium production value that can be believed better than a factor of two.

With regard to hydrogen generation and retention, the most significant observation is that the differences between calculated and measured values are not exceedingly large if recoil and diffusional losses are assumed. The results are reasonably consistent with measurements on alloys of similar materials, and support the fact that a surprisingly large fraction of hydrogen appears to be retained in both pure metals and alloys below ~100 °C. These retention rates indicate that the currently employed cross-sections for hydrogen generation do not necessarily need modification. Although no attempt has been made here to account for diffusional losses, estimates of the average hydrogen diffusion length for the irradiation conditions would suggest that in the absence of defect trapping, even at these low temperatures most of the generated hydrogen should have been lost. Therefore, trapping of the hydrogen at defect clusters and possibly helium sites must play a significant if not controlling role in the hydrogen retention.

Acknowledgements

The authors would like to acknowledge the contributions of Gordon Willcutt at LANL for calculations of sample temperature. This work was supported by the US Department of Energy under the APT program at Los Alamos National Laboratory. Battelle Memorial Institute operates PNNL for the USDOE.

References

[1] APT ^{3}He target/blanket topical report, Los Alamos National Laboratory Report LA-CP-94-27, Rev. 1, 1994.
[2] S.A. Maloy, W.F. Sommer, Proceedings of the Topical Meeting on Nuclear Applications of Accelerator Technology, Albuquerque, NM, 16–20 November 1997, p. 58.
[3] S.L. Green, W.V. Green, F.H. Hegedus, M. Victoria, W.F. Sommer, B.M. Oliver, J. Nucl. Mater. 155–157 (1988) 1350.
[4] M.R. James, S.A. Maloy, W.F. Sommer, P.D. Ferguson, M.M. Fowler, G.E. Mueller, R.K. Corzine, in: J.G. Williams, D.W. Vehar, F.H. Ruddy, D.M. Gilliam (Eds.), Reactor Dosimetry: Radiation Metrology and Assessment, ASTM STP, vol. 1398, ASTM, West Conshohocken, PA, 2001, p. 167.
[5] H. Farrar, B.M. Oliver, J. Vac. Sci. Technol. A 4 (1986) 1740.
[6] B.M. Oliver, F.A. Garner, L.R. Greenwood, J.A. Abrefah, J. Nucl. Mater. 283–287 (2000) 1006.
[7] R.E. Prael, H. Lichtenstein, Los Alamos National Laboratory Report LA-UR-89-3014, 1989.
[8] H.G. Hughes et al., Proceedings of the 2nd International Topical Meeting on Nuclear Applications of Accelerator Technology, Gatlinburg, TN, 20–23 September 1998, p. 281.
[9] A. Gilbert, A.G.W. Cameron, Can. J. Phys. 43 (1965) 1446.
[10] A.V. Ignatyuk, G.N. Smirenkin, A.S. Tishin, Sov. J. Nucl. Phys. 21 (1975) 255.
[11] L.A. Charleton, L.K. Mansur, M.H. Barnett, R.K. Corzine, D.J. Dudziak, M.S. Wechsler, Proceedings of the 2nd International Topical Meeting on Nuclear Applications of Accelerator Technology, Gatlinburg, TN, 20–23 September 1998, p. 247.

[12] M. Enke et al., Nucl. Phys. A 657 (1999) 317.
[13] B.M. Oliver, F.A. Garner, S.A. Maloy, W.F. Sommer, P.D. Ferguson, M.R. James, in: S.T. Rosinski, M.L. Grossbeck, T.R. Allen, A.S. Kumar (Eds.), Effects of Radiation on Materials: 20th International Symposium, ASTM STP, vol. 1405, ASTM, West Conshohocken, PA, 2001, p. 612.
[14] F.A. Garner, B.M. Oliver, L.R. Greenwood, M.R. James, P.D. Ferguson, S.A. Maloy, W.F. Sommer, J. Nucl. Mater. 296 (2001) 66.